

Proton Radii of $^{12-17}\text{B}$ Define a Thick Neutron Surface in ^{17}B

A. Estradé,^{1,2,*} R. Kanungo,^{1,†} W. Horiuchi,³ F. Ameil,² J. Atkinson,¹ Y. Ayyad,^{4,‡} D. Cortina-Gil,⁴ I. Dillmann,^{2,§}
 A. Evdokimov,² F. Farinon,² H. Geissel,^{2,5} G. Guastalla,² R. Janik,⁶ M. Kimura,³ R. Knöbel,² J. Kurcewicz,²
 Yu. A. Litvinov,² M. Marta,² M. Mostazo,⁴ I. Mukha,² C. Nociforo,² H. J. Ong,⁷ S. Pietri,² A. Prochazka,²
 C. Scheidenberger,^{2,5} B. Sitar,⁶ P. Strmen,⁶ Y. Suzuki,^{8,9} M. Takechi,² J. Tanaka,⁷ I. Tanihata,^{7,10} S. Terashima,¹⁰
 J. Vargas,⁴ H. Weick,² and J. S. Winfield²

¹*Astronomy and Physics Department, Saint Mary's University, Halifax, Nova Scotia B3 H 3C3, Canada*

²*GSI Helmholtzzentrum für Schwerionenforschung, D-64291 Darmstadt, Germany*

³*Department of Physics, Hokkaido University, Sapporo 060-0810, Japan*

⁴*Universidad de Santiago de Compostela, E-15706 Santiago de Compostela, Spain*

⁵*Justus-Liebig University, 35392 Giessen, Germany*

⁶*Faculty of Mathematics and Physics, Comenius University, 84215 Bratislava, Slovakia*

⁷*RCNP, Osaka University, Mihogaoka, Ibaraki, Osaka 567 0047, Japan*

⁸*Department of Physics, Niigata University, Niigata 950-2181, Japan*

⁹*RIKEN Nishina Center, Wako, Saitama 351-0198, Japan*

¹⁰*School of Physics and Nuclear Energy Engineering and IRCNPC, Beihang University, Beijing 100191, People's Republic of China*

(Received 11 May 2014; published 23 September 2014)

The first determination of radii of point proton distribution (proton radii) of $^{12-17}\text{B}$ from charge-changing cross sections (σ_{CC}) measurements at the FRS, GSI, Darmstadt is reported. The proton radii are deduced from a finite-range Glauber model analysis of the σ_{CC} . The radii show an increase from ^{13}B to ^{17}B and are consistent with predictions from the antisymmetrized molecular dynamics model for the neutron-rich nuclei. The measurements show the existence of a thick neutron surface with neutron-proton radius difference of 0.51(0.11) fm in ^{17}B .

DOI: 10.1103/PhysRevLett.113.132501

PACS numbers: 21.10.Gv, 25.60.Dz, 21.60.Gx

The finding of a nuclear halo and skin marked the beginning of a new age in nuclear science, breaking down conventional rules [1,2]. These exotic structures in neutron-rich nuclei develop with a nearly pure neutron surface. An intriguing question, therefore, is how the large neutron-to-proton asymmetry in such nuclei influences the proton distribution. The proton radius is of crucial importance in extracting the neutron skin thickness, together with the knowledge on matter radius. The neutron skin thickness provides guidance to constrain the theoretical description of the equation of state of asymmetric nuclear matter which describes the properties of bulk neutron-rich nuclear matter [3]. In addition, the Borromean neutron halo nuclei are unique quantum systems bound as a three-body system with a core nucleus and two halo neutrons, but any two of the components together are not a bound system. In such systems, the proton and matter radii can be used to understand the halo correlation.

Electron scattering on stable nuclei has been the primary source of knowledge for proton distribution [4]. For short-lived nuclei, however, such experiments are still not possible, though developments towards that are under way at RIKEN, Japan [5,6]. Therefore, measurements of charge radii in the light neutron-rich nuclei have been confined to the isotope shift technique [7–10], which, however, is difficult to extend to the drip line. This is

due to the weak beam intensities and limitations from the usually used ISOL production technique.

The total interaction cross section is a reliable method for extracting the root-mean-square (rms) matter radii of nuclei [1,11]. Analogously, the charge-changing cross section (σ_{CC}), which is the sum of all processes that change the proton number of a nucleus, is a potentially useful method to obtain the proton radii of neutron-rich nuclei [12,13]. The σ_{CC} includes charge-exchange cross sections, which are, however, negligibly small as can be understood from the spectrum in Fig. 1(c) as well as estimates in Ref. [14]. In this Letter, we report on the first determination of the rms radii of point proton distributions, i.e., protons as point particles (henceforth referred to as “proton radii”) of $^{12-17}\text{B}$ through precisely measured σ_{CC} at $\sim 900\text{A MeV}$. The results provide the first determination of the extent of the neutron surface thickness in ^{17}B .

Investigations for ^6He [7,8], ^{11}Li [9], and ^{11}Be [10] have shown that the halo leads to an increase in the charge radius. Some of these observations led to the conclusion that in two-neutron halos the neutrons are strongly correlated. In the p - sd shell nuclei, halo formation is associated with the breakdown of the $N = 8$ shell closure. Here, there is an inversion between the $2s_{1/2}$ and $1p_{1/2}$ orbitals. While this is observed in Li and Be isotopes, the B isotopic chain does not show such an inversion for ^{13}B [15]. The presence

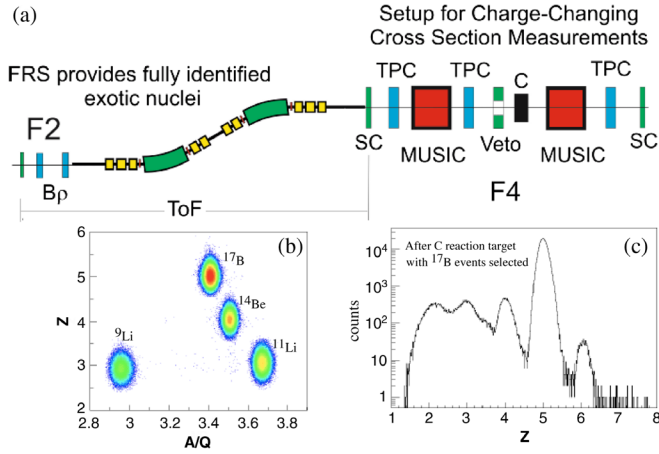


FIG. 1 (color online). (a) Schematic view of the experiment setup at the FRS with detector arrangement at the final focus F4. Identification spectrum of (b) ^{17}B before reaction target and (c) $Z = 5$ after reaction target.

of the ($2s_{1/2}$) orbital is observed in the ground states of $^{14,15}\text{B}$ [16,17]. The effect of the odd neutron in the s orbital is found to increase the charge radius in ^{11}Be [10]. To understand the effect of the s orbital versus pairing and neutron separation energy, a study of $^{14,15}\text{B}$ with an odd proton is important.

The Borromean ^{17}B nucleus draws special interest with discussion of it being a two-neutron halo. This stems from measurements of a moderately narrow momentum distribution [18] and a fairly large matter radius [19,20]. The $2s_{1/2}$ orbital fraction in the ground state extracted from these measurements ranges from 0.17 to 0.89 [18–21], all under the assumption of the ^{15}B core being in the ground state. However, the ^{15}B core has a 33% to 47% probability of being in its $5/2^-$ excited state [22] from the neutron removal reaction measurement in coincidence with gamma detection.

The boron isotopes show cluster structure development in the antisymmetrized molecular dynamics (AMD) framework. The cluster structure in ^{11}B vanishes for the neutron closed-shell nucleus ^{13}B and becomes prominent again with increasing neutron number [23]. The rms matter and proton radii predicted from AMD [24] shows an increase in the proton radius from ^{13}B to ^{17}B . The relativistic mean field calculations [25] predict a nearly constant radius with extremely small increase between ^{15}B and ^{17}B .

We report here the first proton radii measurements for $^{12-17}\text{B}$ from σ_{CC} using the transmission technique. In this method, the number (N_{in}) of incident nuclei AZ , before the reaction target is identified and counted. After the target, the nuclei with the same charge Z is identified and counted event by event ($N_{\text{same}Z}$). The σ_{CC} is obtained from a ratio of these counts and is defined as $\sigma_{\text{CC}} = t^{-1} \ln(R_{T_{\text{out}}}/R_{T_{\text{in}}})$, where $R = N_{\text{same}Z}/N_{\text{in}}$, T_{in} , and T_{out} refer to measurements with and without the reaction target, and t is the thickness of the target. The experiment was performed with the

fragment separator FRS [26] at GSI, Germany. Beams of $^{10,14-17}\text{B}$ and $^{11-13}\text{B}$ were produced by fragmentation of ^{22}Ne and ^{40}Ar primary beams, respectively, interacting with a 6.3 g/cm^2 thick Be target. The isotopes of interest were separated in flight and identified using their magnetic rigidity ($B\rho$), time of flight (F2 to F4), and by the energy loss measured in a multisampling ionization chamber (MUSIC) [27]. The σ_{CC} was measured with a 4.010 g/cm^2 thick carbon reaction target placed at the final focus (F4) (Fig. 1). The MUSIC detector after the reaction target counts $N_{\text{same}Z}$. The Z resolution of this detector was $\sigma = 5.1\%$ for boron.

Information from the detectors in the experimental setup was used to minimize and estimate the contribution of various sources of systematic uncertainties. Beam tracking with time-projection chamber (TPC) detectors [28] provided a definition of the beam spot size and was used to exclude events with large incident angles. The position measured with the TPC after the target provided a measurement of the probability that ions scatter out of the acceptance of the MUSIC. From the latter effect, we estimate a systematic uncertainty from 0.4 to 2.2 mb for different boron isotopes. A veto scintillator placed right in front of the reaction target, with a hole slightly smaller than the target area, provided the condition for rejection of events incident on the edge of the reaction target, as well as for those scattered by nuclear reactions in matter upstream of it. These events are excluded from the incident beam selection and do not contribute to our uncertainty. The contribution of contaminants in the incident beam selection was estimated to be $\approx 2.1 \text{ mb}$, the ratio of the contaminant to nucleus of interest being of the order of 5×10^{-4} . Other sources of systematic uncertainties include the numerical method used to count $N_{\text{same}Z}$ from Fig. 1(c), the background from ions that undergoes a nuclear reaction within this detector, and uncertainty in the target thickness which was $< \pm 0.15\%$. The total systematic uncertainties lie in the range from 2.6 to 3.4 mb for different isotopes.

The measured cross sections for ^{10}B and ^{11}B are $762 \pm 10 \text{ mb}$ and $730 \pm 5 \text{ mb}$, respectively (open triangles in Fig. 2). However, they do not reflect the correct σ_{CC} , as they contain effects besides direct proton removal. This is because ^9B is a proton unbound nucleus. Hence, the one- and two-neutron removal reactions from $^{10,11}\text{B}$, respectively, that are not charge-changing reactions, result in a change in the Z number. Therefore, for $^{10,11}\text{B}$ we subtract the one- and two-neutron removal cross sections (σ_{-n} , σ_{-2n}) to the final states in the residual nucleus that are proton unbound. The σ_{-n} were calculated in the eikonal model framework of the core + neutron model of the nucleus. Spectroscopic factors for the relevant final states of the core were obtained from the $^{10}\text{B}(p, d)^9\text{B}$ and $^{11}\text{B}(p, d)^{10}\text{B}$ transfer reactions [29], which used a plane wave Born approximation (PWBA) analysis. We consider 15% uncertainty in the neutron removal cross section. The difference

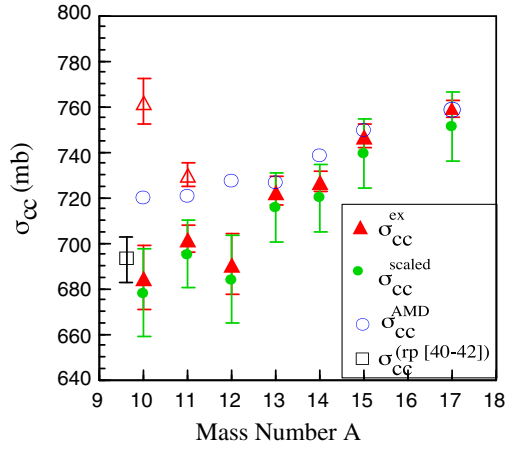


FIG. 2 (color online). The filled triangles for $^{13-17}\text{B}$ are measured σ_{CC} . The open triangles for $^{10,11}\text{B}$ are the measured cross sections. The filled triangles for $^{10-11}\text{B}$ are $\sigma_{\text{CC}}^{\text{corr}}$. The open square is the weighted average value of σ_{CC} calculated using the proton radius of ^{10}B from Refs. [40–42]. The filled circles (green) are $\sigma_{\text{CC}}^{\text{scaled}}$ using $f_{\text{av}}^{\text{all}}$ (see text). The open circles are σ_{CC} using AMD model densities.

in the cross section with spectroscopic factors from the Cohen-Kurath shell model [30] predictions and those reported in the experiment for ^{10}B falls within this uncertainty [29]. The σ_{-n} for proton unbound states in ^{10}B was, therefore, estimated to be 69 ± 10 mb and that for ^{11}B was 19 ± 4 mb. For ^{11}B , there is no shell model result for the highest excited state at 14 MeV which is observed experimentally. A variation of $\sim 20\%$ is found between the results from the shell model and experimental values which is reflected in our uncertainty. There might be a possibility that not all excited states were observed in these (p, d) measurements, and the PWBA analysis is better replaced by a distorted-wave Born approximation analysis. However, shell model predictions and measurements have been looked into for understanding the range of spectroscopic factors. Owing to the rapid increase in the proton separation energy, the neutron removal cross section to proton unbound states decreases sharply moving to the neutron-rich isotopes; hence, those σ_{CC} values do not need to be corrected.

The cross section value for the direct removal of two neutrons σ_{-2n} was taken to be of the order of $\sqrt{\sigma_{-n}^{\text{tot}}}$, where σ_{-n}^{tot} is the sum of neutron removal to all final states of the core nucleus following σ_{-2n} values in Ref. [31]. This is consistent with estimates based on $\sigma_{-2n} = (\sigma_{-n}^{\text{tot}})^2 / \sigma_I$, with σ_I being the interaction cross section. The σ_{-2n} values for $^{10,11}\text{B}$ were estimated to be 8 ± 1 mb and 9 ± 2 mb, respectively.

The experimental values of σ_{CC} are listed in Table I for $^{10-17}\text{B}$. They are shown by (red) filled triangles in Fig. 2 with those for $^{10,11}\text{B}$ being the corrected σ_{CC} . The σ_{CC} of B isotopes has previously been reported by Ref. [32]. The present data have a significantly smaller uncertainty than

TABLE I. Secondary beam energies measured σ_{CC} and the root-mean-square proton and matter radii derived from the data for the boron isotopes.

Isotope	E/A (MeV)	$\sigma_{\text{CC}}^{\text{ex}}$ (mb)	r_p^{ex} (fm)	$r_p^{\text{ex, scaled}}$ (fm)	r_m^{ex} (fm)
^{10}B	925	685(14) ^a	2.32(5) ^b	2.24(10)	
^{11}B	932	702(6) ^a	2.21(2) ^b	2.33(7)	
^{12}B	991	691(13)	2.31(7)	2.28(10)	2.41(3)
^{13}B	897	723(6)	2.48(3)	2.44(8)	2.41(5)
^{14}B	926	727(4)	2.50(2)	2.46(7)	2.52(9)
^{15}B	920	747(5)	2.60(2)	2.56(8)	2.75(6)
^{17}B	862	759(4)	2.67(2)	2.63(7)	3.00(6)

^a $\sigma_{\text{CC}}^{\text{corr}}$ values shown.

^bFrom e^- , π^+ scattering, and muonic x ray.

Ref. [32], in particular, for the most neutron-rich isotopes, and there was no attempt to derive the proton radii in Ref. [32]. In addition, the σ_{CC} values in Ref. [32] are systematically larger than our measurement, as well as larger than the measurement for stable C-Ne isotopes of Ref. [33]. These higher σ_{CC} values are not consistent with known proton radii from electron scattering measurements in stable isotopes. Although σ_{CC} of other nuclei were reported in Refs. [33–35], there was no attempt to derive the proton radii. Therefore, extracting the proton radius from σ_{CC} is a new development.

The present data were interpreted in the framework of the Glauber model. To evaluate the σ_{CC} , we take a standard optical limit approximation,

$$\sigma_{\text{CC}} = \int \int \{1 - |\exp[i\chi(\mathbf{b})]|^2\} d\mathbf{b},$$

where

$$i\chi(\mathbf{b}) = \int_P \int_T \int_i \sum_i \rho_{Pp}^z(\mathbf{s}) \rho_{Ti}^z(\mathbf{t}) \Gamma_{pi}(\mathbf{b} + \mathbf{s} + \mathbf{t}) ds dt.$$

ρ_{Pp} is the proton density of the projectile, and ρ_{Ti} are densities of the proton and neutron ($i = p, n$) in the target. Γ is the profile function [36]. The reaction cross sections are calculated with another expression called the nucleon-target formalism in the Glauber model [37], which has been applied to several stable and unstable nuclei [38,39].

We use a harmonic oscillator density reproducing the measured charge radius of ^{12}C from electron scattering to calculate the σ_{CC} within the framework of Glauber model. The calculated σ_{CC} of 730 mb is in good agreement with our measured value of 734 ± 6 mb. This supports the present formalism to extract proton radii from the σ_{CC} . It may be noted that unlike what was recently reported in Ref. [13], we did not require any scaling of the experimental cross section to reproduce the known charge radius of ^{12}C . One reason for this is because we performed

finite-range Glauber model calculations in contrast to the zero-range calculations in Ref. [13].

The rms charge radii values for ^{10}B from electron scattering measurements are 2.42(12) fm [40] and 2.58(7) fm [41] and that from muonic x rays is 2.44(6) fm [42]. The point proton radii of ^{10}B extracted using the expression in Ref. [10] from the above values are 2.27(14) fm, 2.41(8) fm, and 2.26(7) fm, respectively. The σ_{CC} calculated in the Glauber model framework with harmonic oscillator density using these point proton rms radii of ^{10}B are 683(27) mb, 710(16) mb, and 681(13) mb, respectively. The calculated values are in close agreement with the experimental ones (Table I, $\sigma_{\text{CC}}^{\text{corr}}$). The ratio of the experimental cross section to the weighted average of the three calculated values yields a normalization factor of $f_{\text{av}} = \sigma_{\text{CC}}^{\text{ex}} / \sigma_{\text{CC}}^{\text{Glauber}} = 0.99 \pm 0.02$. The rms charge radius of ^{11}B is known from π^+ scattering to be 2.40(2) fm [43] (using ^{12}C charge radius as 2.47 fm), from muonic x-rays studies to be 2.38(4) fm [42], and from electron scattering to be 2.42(12) fm [40]. This yields a weighted average point proton radius of 2.21(2) fm. The calculated σ_{CC} with harmonic oscillator density for this radius is 674(6) mb. The average scaling factor and its standard deviation obtained from $^{10,11}\text{B}$, $f_{\text{av}}^{\text{all}}$ is 1.01 ± 0.02 . While within uncertainties this scaling factor is in agreement with that (1.05 ± 0.03) in Ref. [13], it may be noted, however, that the scaling factor using ^{10}B radii from Refs. [40,42] is unity. The $\sigma_{\text{CC}}^{\text{scaled}}$ are (Fig. 2, filled circles) consistent with the $\sigma_{\text{CC}}^{\text{ex}}$.

The rms proton radii of $^{12-17}\text{B}$ were determined from a Glauber model analysis of $\sigma_{\text{CC}}^{\text{ex}}$ using harmonic oscillator density for the protons. The radii are extracted by fitting the $\sigma_{\text{CC}}^{\text{ex}}$ using densities with varying oscillator widths. The resulting point proton radii (r_p^{ex}) are listed in Table I and shown in Fig. 3 by the red filled triangles. Since proton radii from electron scattering for both ^{12}C and ^{10}B can explain $\sigma_{\text{CC}}^{\text{ex}}$ values without any scaling, we have, therefore, extracted the radii from $\sigma_{\text{CC}}^{\text{ex}}$. The radii from $\sigma_{\text{CC}}^{\text{scaled}}$ following the same procedure are listed in Table I for completeness as $r_p^{\text{ex,scaled}}$ and are consistent with (r_p^{ex}). A gradual increase in r_p^{ex} is observed from ^{12}B to ^{17}B . Although ^{14}B has a neutron occupying the $2s_{1/2}$ orbital, there is an attractive interaction between the unpaired proton and the neutron which might hinder a large enhancement of matter and proton radius.

The σ_{CC} , proton radii (r_p^{AMD}), and rms matter radii (r_m^{AMD}) calculated using the densities predicted by the AMD formalism are shown in Figs. 2 and 3. The AMD calculations are performed as described in Ref. [44]. The Gogny D1S effective interaction is used to obtain the basis wave functions of boron isotopes. The ground-state wave functions are described by the superposition of those basis wave functions employing the matter quadrupole deformation as the generator coordinate. The open circles in Fig. 2 show σ_{CC} using r_p^{AMD} . A comparison of the measured radii with r_p^{AMD} exhibit good agreement for neutron-rich

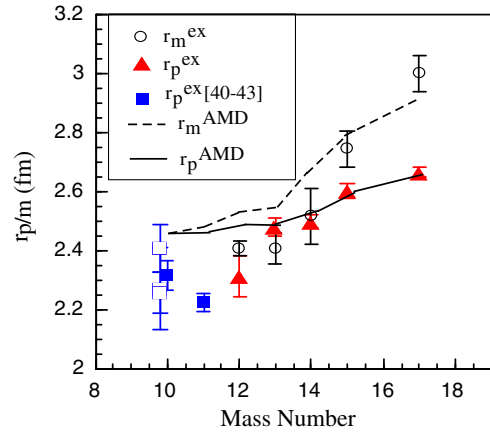


FIG. 3 (color online). The filled triangles for $^{12-17}\text{B}$ are proton radii extracted from $\sigma_{\text{CC}}^{\text{ex}}$ through a Glauber model analysis with harmonic oscillator density. The open squares are proton radii determined from measured charge radii from Refs. [40–42]. The filled square for ^{10}B is the weighted average of the open squares. The filled square for ^{11}B is the radius derived from the measured charge radius from Ref. [43]. The open circles are r_m^{ex} . The solid/dashed lines are $r_p^{\text{AMD}}/r_m^{\text{AMD}}$.

isotopes (Fig. 3) implying the development of cluster structure and deformation with growing neutron excess. The trend is unlike relativistic mean field theory [25] predictions.

We extracted the matter radii from interaction cross section data (σ_T^{ex}) [11,19] through the finite-range Glauber model analysis using harmonic oscillator densities for protons and neutrons. For ^{15}B , we used the interaction cross section value of 1000(20) mb [11]. The r_p^{ex} values were used to describe the proton density. The harmonic oscillator width of the neutron density was then varied to reproduce σ_T^{ex} . The resulting matter radii (r_m^{ex}) are shown in Fig. 3 and listed in Table I. The uncertainties in r_m^{ex} arise from the range of harmonic oscillator radii that give calculated cross sections overlapping with the measured cross section.

The neutron rms radius (r_n^{ex}) derived from r_m^{ex} and r_p^{ex} for ^{17}B is 3.12(7) fm, which leads to a thick neutron surface $r_n^{\text{ex}} - r_p^{\text{ex}}$, of 0.45(8) fm. The proton radius $r_p^{\text{ex,scaled}}$ gives surface thickness of 0.51(11) fm, consistent with that using r_p^{ex} . In a ^{15}B core plus two-neutron model of ^{17}B , the distance between the core and center of mass of the two neutrons (R_{cn}) following Ref. [2] is found to be 5.01(36) fm using r_p^{ex} and 5.12(1.33) fm using $r_p^{\text{ex,scaled}}$. This lies in between the R_{cn} for ^6He [3.84(6) fm [2]] and ^{11}Li [6.20(50) fm [2]]. It is close to that for ^{12}Be [5.11(17) fm, using charge radius from Ref. [45]]. With the central values of the matter and proton radii, one obtains the root-mean-square distance between the two neutrons $r_{\text{nn}} < 0$, which is an unphysical condition. This could point towards the presence of a modified ^{15}B core. The same is also observed for ^{12}Be . This is unlike the cases for ^6He and ^{11}Li . This is probably because there is considerable admixture of the

$d_{5/2}$ orbital together with the $2s_{1/2}$ in ^{17}B and, with $2s_{1/2}$ plus $1p_{1/2}$ orbitals in ^{12}Be . Within the uncertainty bands of the present data, $r_{\text{nn}} > 0$ is obtained only when the matter radii of ^{15}B and ^{17}B are at the lower and upper error bar limits, respectively. In this condition, with central values of $r_p^{\text{ex.scaled}}$ we get $r_{\text{nn}} = 2.94$ fm. That would be comparable to a deuteron-like correlation between the two neutrons.

In summary, the proton radii of the $^{12-17}\text{B}$ nuclei have been derived for the first time from the measured σ_{CC} in the framework of the Glauber model. The radii show a continuous increase with growing neutron-proton asymmetry, consistent with AMD model predictions. The new data suggest a 0.51(11) fm thick neutron surface in ^{17}B . A comparison of the proton and neutron radii between ^{17}B and ^{15}B indicates a ^{15}B core modification in ^{17}B . In comparison with proton radii from electron scattering for ^{10}B and ^{12}C , it is found that the σ_{CC} data are consistent with a scaling factor of near unity, unlike that observed in Ref. [13].

The authors are thankful for the support of the GSI accelerator staff and the FRS technical staff for an efficient running of the experiment. The support from NSERC, Canada for this work is gratefully acknowledged. R. K. thankfully acknowledges the HIC-for-FAIR program and JLU-Giessen for supporting part of the research stay. The support of the People's Republic of China government and Beihang University under the Thousand Talents Program is gratefully acknowledged. The experiment is partly supported by the grant-in-aid program of the Japanese government under the Contract No. 23224008. Discussions with Y. Kanada-Enyo are gratefully acknowledged by R. K.

*Present address: University of Edinburgh, Edinburgh, United Kingdom.

†ritu@triumf.ca

‡Present address: RCNP, Osaka University, Mihogaoka, Ibaraki, Osaka, Japan.

§Present address: TRIUMF, Vancouver, Canada.

[1] I. Tanihata, H. Hamagaki, O. Hashimoto, Y. Shida, N. Yoshikawa, K. Sugimoto, O. Yamakawa, T. Kobayashi, and N. Takahashi, *Phys. Rev. Lett.* **55**, 2676 (1985).
 [2] I. Tanihata, H. Savajols, and R. Kanungo, *Prog. Part. Nucl. Phys.* **68**, 215 (2013).
 [3] J. M. Lattimer, *Annu. Rev. Nucl. Part. Sci.* **62**, 485 (2012).
 [4] I. Sick *et al.*, *Prog. Part. Nucl. Phys.* **47**, 245 (2001).
 [5] T. Suda *et al.*, *Phys. Rev. Lett.* **102**, 102501 (2009).
 [6] M. Wakasugi *et al.*, *Nucl. Instrum. Methods Phys. Res., Sect. B* **317**, 668 (2013).
 [7] L.-B. Wang *et al.*, *Phys. Rev. Lett.* **93**, 142501 (2004).
 [8] P. Mueller *et al.*, *Phys. Rev. Lett.* **99**, 252501 (2007).
 [9] R. Sánchez *et al.*, *Phys. Rev. Lett.* **96**, 033002 (2006).
 [10] W. Nörtershäuser *et al.*, *Phys. Rev. Lett.* **102**, 062503 (2009).

[11] A. Ozawa, T. Suzuki, and I. Tanihata, *Nucl. Phys.* **A693**, 32 (2001).
 [12] I. Tanihata *et al.*, *Nucl. Instrum. Methods Phys. Res., Sect. A* **532**, 79 (2004).
 [13] T. Yamaguchi, I. Hachiuma, A. Kitagawa, K. Namihira, S. Sato, T. Suzuki, I. Tanihata, and M. Fukuda, *Phys. Rev. Lett.* **107**, 032502 (2011).
 [14] L. S. Celenza, J. Hüfner, and C. Sander, *Nucl. Phys.* **A276**, 509 (1977).
 [15] H. Y. Lee *et al.*, *Phys. Rev. C* **81**, 015802 (2010).
 [16] V. Guimaraes *et al.*, *Phys. Rev. C* **61**, 064609 (2000).
 [17] E. Sauvan *et al.*, *Phys. Rev. C* **69**, 044603 (2004).
 [18] T. Suzuki *et al.*, *Phys. Rev. Lett.* **89**, 012501 (2002).
 [19] T. Suzuki *et al.*, *Nucl. Phys.* **A658**, 313 (1999).
 [20] Y. Yamaguchi *et al.*, *Phys. Rev. C* **70**, 054320 (2004).
 [21] H. T. Fortune and R. Sherr, *Eur. Phys. J. A* **48**, 103 (2012).
 [22] R. Kanungo *et al.*, *Phys. Lett. B* **608**, 206 (2005).
 [23] Y. Kanada-Enyo and H. Horiuchi, *Phys. Rev. C* **52**, 647 (1995).
 [24] Y. Kanada-Enyo and M. Kimura, *Phys. Rev. C* **72**, 064301 (2005).
 [25] G. Lalazissis, C. D. Vreternar, and P. Ring, *Eur. Phys. J. A* **22**, 37 (2004).
 [26] H. Geissel *et al.*, *Nucl. Instrum. Methods Phys. Res., Sect. B* **70**, 286 (1992).
 [27] A. Stolz *et al.*, *Phys. Rev. C* **65**, 064603 (2002).
 [28] V. Hlinka, M. Ivanov, R. Janik, B. Sitar, P. Strmen, I. Szarka, T. Baumann, H. Geissel, and W. Schwab, *Nucl. Instrum. Methods Phys. Res., Sect. A* **419**, 503 (1998).
 [29] D. Bachelier, M. Bernas, I. Brissaud, C. Détraz, and P. Radvanyi, *Nucl. Phys.* **A126**, 60 (1969).
 [30] S. Cohen and D. Kurath, *Nucl. Phys.* **A101**, 1 (1967).
 [31] N. Kobayashi *et al.*, *Phys. Rev. C* **86**, 054604 (2012).
 [32] L. V. Chulkov *et al.*, *Nucl. Phys.* **A674**, 330 (2000).
 [33] W. R. Webber, J. C. Kish, and D. A. Schrier, *Phys. Rev. C* **41**, 520 (1990).
 [34] B. Blank *et al.*, *Z. Phys. A* **343**, 375 (1992).
 [35] L. Chulkov *et al.*, *Nucl. Phys.* **A603**, 219 (1996).
 [36] B. Abu-Ibrahim, W. Horiuchi, A. Kohama, and Y. Suzuki, *Phys. Rev. C* **77**, 034607 (2008).
 [37] B. Abu-Ibrahim and Y. Suzuki, *Phys. Rev. C* **61**, 051601(R) (2000).
 [38] W. Horiuchi, Y. Suzuki, B. Abu-Ibrahim, and A. Kohama, *Phys. Rev. C* **75**, 044607 (2007).
 [39] W. Horiuchi, T. Inakura, T. Nakatsukasa, and Y. Suzuki, *Phys. Rev. C* **86**, 024614 (2012).
 [40] T. Stovall, J. Goldemberg, and D. B. Isabelle, *Nucl. Phys.* **A86**, 225 (1966).
 [41] A. Cichocki, J. Dubach, R. Hicks, G. Peterson, C. de Jager, H. de Vries, N. Kalantar-Nayestanaki, and T. Sato, *Phys. Rev. C* **51**, 2406 (1995).
 [42] A. Olin, P. R. Poffenberger, G. A. Beer, J. A. MacDonald, G. R. Mason, R. M. Pearce, and W. C. Sperry, *Nucl. Phys.* **A360**, 426 (1981).
 [43] B. M. Barnett *et al.*, *Phys. Lett.* **97B**, 45 (1980).
 [44] M. Kimura *et al.*, *Phys. Rev. C* **69**, 044319 (2004).
 [45] A. Kreiger *et al.*, *Phys. Rev. Lett.* **108**, 142501 (2012).